Delft University of Technology
Department of Aerospace Engineering

Report LR-375

FATIGUE CRACK GROWTH OF CORNER CRACKS IN LUG SPECIMENS

S. Friedrich and J. Schijve

Delft - The Netherlands

January 1983

Delft University of Technology
Department of Aerospace Engineering

Report LR-375

FATIGUE CRACK GROWTH OF CORNER CRACKS IN LUG SPECIMENS

S. Friedrich*) and J. Schijve

*) Research Fellow 1981/82, on leave from the Israel Aircraft Industries

Delft - The Netherlands January 1983

ABSTRACT

Constant-amplitude tests and simplified flight-simulation tests with one peak load per flight were carried out on 7075-T6 lug specimens. Corner cracks at the pin-loaded hole were initiated by a small starter notch. Application of marker loads indicated successive locations of the crack front on the fracture surfaces. These indications gave information about crack shape development and crack growth rates along the crack front. The latter data were used to determine empirical stress intensity factors, which were compared to calculated data. Damage calculations gave indications on crack growth retardation of corner cracks.

NOTATIONS

a	crack depth along the hole
c	crack length along the surface
CA	constant-amplitude
D	hole diameter
F	correction factors
K	stress intensity factor
ℓ	crack length (Fig. 8)
m	number of cycles per flight
n	number of cycles
N_2	crack growth life until c = 2 mm
N_t	crack growth life until failure
P	pin load
R	- stress ratio = S_{min}/S_{max}
	- hole radius (D/2)
S	net stress
S_g	stress at ground level
S_{OL}	stress at peak load (Over Load)
S_p	nominal bearing pressure on hole
t	thickness
W	lug width
θ,θ'	polar angles (Fig. 8)

CONTENTS

1 INTRODUCTION

Fatigue cracks in aircraft structures usually occur in joints of various types (bolted, riveted, lugs). In the joint the crack frequently starts at a hole loaded by a bolt or a rivet. A large part of the fatigue life is then covered by crack growth from a very small size to a size comparable to the hole diameter or the material thickness. Quite often the crack nucleates as a small "part-through crack", i.e. it starts as a small corner crack or as an embedded semi-elliptical crack inside a hole. At a later stage the crack has grown through the full thickness to become a well recognized "through crack". Because the growth from an initially small part-through crack to a visible through crack covers a substantial part of the fatigue life, the prediction of the life involved is generally considered to be a technically relevant problem. This has been greatly emphasized by the so-called damage tolerance requirements [1]. The prediction is a complex problem in view of the curvature of the crack front. As a result the stress intensity factor K will vary along the crack front. The problem received considerable interest in the literature, especially with respect to calculating and estimating K variations along a curved crack front. The number of empirical verifications for loaded holes, however, is not too large, and this was the starting point for the present investigation.

Fatigue tests were carried out on lug specimens provided with a very small corner notch to initiate crack growth. A lug type specimen was chosen for two reasons:
(1) A lug has a simple geometry with a well defined load transmission as compared to bolted and riveted joints. In the latter types of joints load transmission partly occurs by frictional forces between the plates which are clamped by the fasteners.
(2) Lugs occur at various locations in an aircraft structure, either for easy assembling of major components, or for the possibility of rotation (e.g. landing gears, control rods). In such cases cracks in a lug can lead to fail-safe problems, and information on crack growth behaviour is important.

Tests were carried out on simple lug specimens as shown in Figure 1, which also illustrates the load sequences applied. In all tests batches of small marker load cycles were applied in order to produce growth bands on the fracture surfaces. The bands indicate the development of the crack shape during a test. The comstant-amplitude (CA) tests were carried out to compare the crack growth rate along the crack front with predictions based on through-crack data and K-values derived from the literature. Secondly the CA tests served as a reference to the simplified flight-simulation tests (type II and III in Fig. 1). The latter tests were made to see if overloads (OL) or "underloads" (i.e. ground-to-air cycles) would affect crack front shapes. Another reason was to observe crack growth interaction effects (growth delays or accelerations) on the behaviour of a corner crack. For this purpose simple but systematic variations of the load history were applied. Especially the application of an overload at the beginning of a flight (type II) or at the end of a flight (type III) was considered to be of interest. The effect might be different for a short flight (m = 5) and for a long flight (m = 100)

The present report starts with a description of experimental details and a presentation of test results, including fractography of the marker load bands. Crack growth rates along the cfack front are deduced from these bands and these growth rates are used to obtain empirical K values. The latter data are compared to calculated K data derived from the literature. The data of the flight-simulation tests are used to indicate possible interaction effects. The report is completed by a discussion and conclusions.

2 EXPERIMENTAL DETAILS

Specimens

The double-ended lug type specimens (see Figure 1) were cut from 7075-T6 bare plate material of 9.6 mm thickness. The holes were drilled with reaming as a final treatment. The diameter of the hole is 25 mm with tolerance limits 25.000 and 25.021 mm. The hole was loaded by a low-alloy steel pin with tolerance limits 25.000 mm and 24.979 mm. This gives a neat fit.
Each hole was provided with a single crack initiation notch at one corner of the hole. The crack initiation notch was produced by electrical discharge machining (EDM), the shape of the notch being triangular with edges as small as 0.25 mm (see Fig. 1). The notches were made at different sides of the two holes and at opposite sides of the plate thickness. The specimens were loaded in the rolling direction. Mechanical properties of the material are shown in Figure 1.

Test set-up

Each end of a specimen was mounted in a fork with a hardened steel pin, see Figure 2. The forks were fixed in the hydraulic clampings of the fatigue machine. The forks were provided with slots to allow visual crack growth observations during the test. If one lug end of a specimen had failed the fracture surface was removed from the specimen. The broken end was clamped in the fatigue machine to continue the test on the other lug end. As a result two data sets were obtained from each specimen.
The fatigue machine was an electrohydraulic 200 kN Amsler testing machine with MTS electronics. Load-control occurred by a PDP-11/04 computer.
Special programs were written by P. Kempen to obtain the required load histories.
The cyclic frequency of the loads was 10 Hz, but the marker loads were applied at 30 Hz.

Load histories and marker loads

A survey of the tests is given in Figure 1, which includes the specimen identification number. All stresses indicated are net stresses on the critical section of the lug. In general only one specimen was tested for each combination of variables, but it should be remembered that each specimen contains two lug ends.

The marker loads were applied to indicate crack front positions on the fracture surface. The load sequence during one block of marker loads is indicated in Figure 3. This produces bands on the fracture surface as shown in Figure 4.
The stress levels adopted for the marker loads were based on experience of Minderhoud [2] during a previous investigation on corner cracks at open unloaded holes in specimens of the same material. The marker loads had the same maximum stress as the load history of the test. The stress range was ΔS = 15 MPa, although occasionally ΔS = 10 MPa was applied. The number of marker load cycles in one block had to be adjusted to the needs of the test. The criterion was to minimize the crack extension during the marker loads, without spoiling the visibility of the marker bands on the fracture surfaces. In almost all tests the number was 40 000 cycles, but 60 000 cycles were applied in a few tests. It was shown by Minderhoud [2] that the marker loads had a negligible effect on crack growth. Blocks of marker loads were applied at selected intervals in order to obtain some 6 to 10 bands in each fracture surface.

Crack growth observations and fractography

Visual observations during a test could only be made on the outside surface by watching the crack through the slots in the forks (Fig. 2). Around the hole of the lug ends a grid of concentric circles (spacing 1 mm) was photographically etched on the specimen surfaces. The grid was used for visual crack length measurements. An example of the crack growth curves obtained in this way is shown in Figure 5.

The marker bands on the fracture surfaces were recorded in an optical profile measuring machine. In this machine the fracture surface was projected on tracing paper, employing a magnification of 10 times. The positions of the bands were copied on the paper, and the pictures thus obtained were used for further evaluation of crack growth along the crack front. Examples of such pictures are shown in Figure 7.

3 TEST RESULTS AND NUMERICAL TREATMENT OF THE DATA

Visual crack growth data

Full tabular data have been collected in a separate document [3]. As an illustration data of one specimen are plotted in Figure 5. Similar graphs were made for all specimens and from such graphs the fatigue life (N_2) until a crack length c = 2 mm was derived. If N_t is the total life until failure the crack growth life from 2 mm to failure is obtained as $N_t - N_2$. The value c = 2 mm was adopted because for lower c-values observations were not always succesful, or the growth data were still somewhat erratic. A compilation of N_t, N_2 and $N_t - N_2$ data is given in table 1. The results are plotted in Figure 6.

Fractographic observations

Several examples of successive crack front locations are shown in Figure 7. There is a good deal of similarity between crack front shapes of different specimens. Generally the crack depth (a) along the hole is slightly larger than the crack length (c) along the surface. In many cases aspect ratio's (a/c) are between 1.1 and 1.2. Because a/c is only slightly larger than 1 the crack growth is almost a concentric and circular crack extension.

One systematic deviation of the similarity of crack front shapes can be observed. For a higher maximum stress in the test (either S_{max} for CA-loading or S_{OL} for flight-simulation loading) the crack front at the plate surface and the surface of the hole is bending backwards, see left sketch in Figure 8. This will be discussed later.

The marker bands were also used for the determination of crack growth rates. In view of crack front bending at the free surface the definition of a and c is somewhat ambiguous. For that reason the growth rate was measured at three "interior" points of the crack front, indicated by angles $\theta' = 22.5°$, 45° and 67.5° respectively (see Figure 8). The growth rate was calculated as:

$$\frac{d\ell}{dn} = \frac{\Delta\ell}{\Delta n} \qquad (1)$$

with $\Delta\ell$ being the perpendicular distance between the marker bands, and Δn the number of load cycles applied between two blocks of marker loads. This growth

rate was supposed to apply to a crack length ℓ midway between the marker loads. Plots of $d\ell/dn$ as a function of ℓ were made for all specimens. Some examples are presented in Figure 9 (U and L in the specimen identification number refer to upper lug and lower lug respectively). It was generally observed that $d\ell/dn$ was not very much different for the three θ-values. Actually a constant da/dn along the crack front requires that the shape becomes circular which is only approximately true (a/c slightly larger than one).

Figure 9 shows that $d\ell/dn$ is a slowly increasing function of crack length. In view of this consistent crack extension behaviour the crack growth life $(N_t - N_2)$ is also characteristic for the growth rate development.

Empirical K-values

Empirical K-values can be derived from the crack growth data of the fatigue tests with constant-amplitude loading (Fig. 9a). This is possible because the relation between the crack growth rate (da/dn) for through cracks and ΔK is available from a previous test series [2]. Those results obtained at R = 0.1 and R = 0.5 are well approximated by:

$$da/dn = 2.3 \times 10^{-6} \, (\Delta K_{eff})^{2.75} \qquad (2)$$

with da/dn in mm/cycle and ΔK_{eff} in MPa$\sqrt{m}$, and:

$$\Delta K_{eff} = U \, \Delta K \text{ with } U = 0.55 + 0.33 \, R + 0.12 \, R^2 \qquad (3)$$

With these equations the da/dn-results of Figure 9a were converted into $\Delta K/\Delta S$-values. For specimen 2 the stress ratio is positive (R = 40/100), whereas for specimen 17 it is negative (R = -40/160). However, for a lug loaded in compression the critical minimum section remains practically unstressed [4]. Consequently, the data for specimen 17 are treated as if $S_{min} = 0$ and thus: R = 0 and ΔS = 160 MPa. The $\Delta K/\Delta S$ results are presented in Figure 10. Although there is scatter the general trend is the same for the two specimens loaded at a low and a high stress amplitude respectively. Only the result of the first crack front of specimen 2 are too high. It follows from fracture mechanics that the same crack front shape development at any fatigue load requires that the same $\Delta K/\Delta S$ should be found. This appears to be in reasonable agreement with the results in Figure 10.

The average $\Delta K/\Delta S$-ℓ curve of Figure 10 is transformed in a geometry correction factor F as a function of a, where F is defined by:

$$K = F \, S_p \sqrt{\pi a} \qquad (4)$$

In the definition the nominal bearing pressure on the hole (S_p) is adopted as the characteristic stress in view of a comparison to calculated data to be made later. Because ΔS is a nominal net section stress:

$$S(W-D) = S_p \, D \qquad (5)$$

and Eq. (4) can be rewritten as:

$$F = \frac{K}{S_p \sqrt{\pi a}} = \left(\frac{\Delta K}{\Delta S}\right) \frac{D}{(W-D)\sqrt{\pi \ell (a/\ell)}} \qquad (6)$$

with:

$$a/\ell = a/c \left[\cos^2\theta + \left(\frac{a}{c}\right)^2 \sin^2\theta\right]^{-1/2} \quad \text{(see Fig. 8)}$$

The curves obtained for three polar angles θ are shown in Figure 11. They apply to a/c = 1.15 which is a characteristic mean value for the present tests. Figure 11 shows a weak dependence on θ.

Comparison between empirical K-values and calculated data

Raju and Newman [5] made finite-element calculations for two symmetrical corner cracks at holes in very wide panels, both for open holes in panels under tension and for panels with wedge-loaded holes. By superpositon of these two cases the solution of a pin-loaded hole can be obtained. The Raju/Newman data apply to a/c = 0.2, 1 and 2, to a/t = 0.2, 0,5 and 0.8 and to R/t = 0.5 and 1.0. Consequently interpolations have to be made to arrive at dimensional ratio's of the present tests. For R/t it even requires an extrapolation because here R/t = 12.5/9.6 = 1.30. Moreover, a width correction has to be introduced, as well as a correction factor for having only one corner crack instead of the two symmetrical corner cracks of the Raju/Newman data. The interpolation procedures are summarized in Appendix A. The results are presented in Figure 11. The agreement with the empirical results is not satisfactory.

Damage calculations

In this report non-interaction damage calculations will be made only. The purpose is to see whether damage interaction effects would become apparent as large deviations from $\Sigma n/N = 1$. According to the range-pair count method (also rain-flow count method) each flight of type II and type III consists of one large cycle between S_g and S_{OL} (Fig. 1), and (m-1) smaller gust cycles between S_{min} = 40 MPa and S_{max} = 120 MPa. As a result there are only three different magnitudes of load cycles to be considered: (1) S_{min} = 40, S_{max} = 120 (gust cycles), (2) S_{min} = 0 and S_{max} = 160 (low S_{OL}) and (3) S_{min} = 0 and S_{OL} = 200 (high S_{OL}). It should be noted that the compression part of the larger cycles (2) and (3) is again ignored, because it leaves the critical minimum section practically unstressed. In Appendix B it is analysed whether the mean values of $N_t - N_2$ in table 1 are a mutually consistent data set. This is done by considering the crack growth relations of Eqs. (2) and (3). It turned out that the crack growth life for cycles (1) and (2) are in excellent agreement, whereas the life for cycle (3) was longer than expected. Since there are no reasons to see why this test result should not be valid the mean results of Table 1 were used for calculating $\Sigma n/N$ for the tests of type II and III. With:

$$\Delta = \text{damage per flight} = \frac{m-1}{(N_t - N_2)_{gusts}} + \frac{1}{(N_t - N_{0.2})_{OL}}$$

and thus: Δ/m = average damage per cycle

the result for tests of type II and III is:

$$\text{predicted life} = \frac{1}{\Delta/m} \quad \text{(cycles)}$$

and:

$$\Sigma n/N = \frac{\text{test life}}{\text{predicted life}}$$

Calculated results are presented in Table 2 and Figure 6. If S_{OL} and m are the same for tests of type II and III the predicted lives are also the same. Six $\Sigma n/N$-values are between 0.9 and 1.5, which does not point to significant interaction effects. Four $\Sigma n/N$-values are between 2.6 and 3.1. In the latter cases S_{OL} = 200 and n = 100. Apparently significant interaction effects occurred for these test conditions.

More detailed predictions for crack growth rates under type II and type III loading could have been made. However, in view of the consistent crack growth behaviour in all tests (see discussion on Fig. 9) similar trends as reported for $\Sigma n/N$-values would be found.

4 DISCUSSION

Fatigue crack growth of a corner crack in a lug

In the present tests the shape of the crack front during crack growth was studied by applying marker loads. It turned out that the variation of the crack depth to crack length ratio (a/c) was small. Generally the crack depth (a) was somewhat larger than the crack length at the surface (c), with a/c $\sim$ 1.15 as a mean value.
The crack growth rates along the crack front deduced from the marker loads, were used to obtain empirical K-values as shown in Figures 10 and 11. According to Fig. 11 the variation of K along the crack front is not large. The comparison with calculated data derived from results published by Raju and Newman [5] is not satisfactory as shown in Figure 11. There are several reasons to explain the differences. Raju and Newman analysed very wide and high panels (as compared to the hole diameter). Their dimensions were considerably different from the geometry of the present lug. Various interpolations and extrapolations, and several correction factors had to be applied before the Raju/Newman data could be applied to the dimensions of the lug tested here. Probably the differences were too large to justify the application. A lug is not a long strip, on the contrary the height of the lug head (40 mm, see Fig. 1) is smaller than the lug width (60 mm). Zatz, Eidinoff and Armen [6] have shown the significance of the shape and the size of the lug head for the stress intensity of a through crack. It should be concluded that there is still an apparent need for data on K-factors along the crack front of corner cracks in lugs. At the same time it cannot be overlooked that K for such cracks will depend on the bearing pressure distribution over the bore of the hole and on the occurrence of tangential friction inside the hole as a result of fretting. Recently Hsu [7] has shown that for a lug the pressure distribution is considerably depending on the crack length. Apparently such problems can be analysed by finite-element calculations. At the same time more extensive empirical data on corner crack growth would also be most welcome to check the relevance of calculated results.

Free surface effect on corner crack growth

One systematic trend was observed about the two ends of the crack front at the free surfaces. Apparently crack growth is lagging behind near the free surface, and this was more clear if the maximum stress of the test was higher. In Figure 7a this is observed for constant-amplitude loading and in Figure 7c for flight-simulation loading. The delayed crack growth near the surfaces is also clear in Figure 7d which applies to the highest maximum stress of the present test series. A similar effect of the stress level on crack front

shapes was observed by Hodulak et al [8]. As an explanation they refer to the plane stress situation at the free surface and the plane strain condition inside the material. The plane stress region is associated with a higher crack growth resistance.

The larger plastic zone in the plane stress region will cause more crack closure. This surface phenomenon was experimentally confirmed for through cracks [9, 10]. It should be expected to be applicable to corner cracks as well. Apart from the difference in crack closure there will also be a difference in the maximum stress in the plastic zones at the surface and further inwards. The magnitude of the maximum tensile stress in the shaded areas of Figure 8 will be in the order of the yield stress, but it will be significantly higher in the plane strain plastic zone area along the major part of the crack front. As a result the driving force for crack extension is lower near the surface of the material. The higher stress occurring at the interior can be alleviated at the free surface by more plastic deformation. Consequently the crack front will be lagging behind at the surface. It is thought to be fundamentally the same mechanism, that controls the wellknown tongue-shaped growth bands on the fatigue fracture surfaces of high strength aluminium alloys [11]. Such bands were shown to be the result of quasi-static crack extension during a high peak load as part of a variable-amplitude load history. A large crack extension at the interior goes together with an apparently restrained extension at the surface.

Damage interaction effects

One of the prime reasons for the present investigation was to see whether fatigue damage interaction effects (crack growth retardations and accelerations) would occur in a similar way as they are found for through cracks. A very much similar test program has recently been carried out in the Aerospace Department in Delft. In this program also type II and III fatigue load histories were applied to study the growth of through cracks in 2024-T3 sheet specimens of 2 mm thickness. The results will be published shortly. It turned out that the trends as illustrated by Figure 6 were very much similar for through cracks and the part through cracks studied here.

When planning the present program is was expected that the once per flight load cycle between S_g (ground load) and S_{OL} (peak load) would highly predominate the crack extension. Its own contribution to crack extension would probably be similar as in a constant-amplitude test, but it might well reduce the crack growth during the smaller gust cycles. If so, $\Sigma n/N$-values should exceed 1, especially if the number of gust cycles per flight is large (m = 100). This has been found indeed for S_{OL} = 200 MPa ($\overline{\Sigma n/N} = 2.8$), but it is less evident for S_{OL} = 160 MPa ($N = 100 \rightarrow \overline{\Sigma n/N} = 1.35$). It was also expected that type II loading with the peak load as the first cycle of the flight would produce systematically longer crack growth lives than type III loading, where the peak load occurs in the last cycle of the flight. Although the crack growth lives for type II loading are larger in the three out of four cases (Fig. 6 and Table 2). The differences are not convincing. This result should be a question of further concern, especially if new crack growth models for variable-amplitude loading are to be checked. Attention to this aspect will be given in a future report.

5 SUMMARY AND CONCLUSIONS

In the present investigation lugs of 7075-T6 material were fatigue tested under constant-amplitude loading and simplified flight-simulation loading. In the flight-simulation tests 4 or 99 smaller cycles were applied to which one peak load was added either at the beginning of the flight or at the end. Corner cracks at the holes were initiated from a small starter notch. Crack front locations could be indicated on the fracture surfaces by applications of marker loads. The results and conclusions are summarized below.

1. By the marker load technique information about crack front locations was obtained. It turned out that in most cases the crack depth (a) along the bore of the hole was slightly ahead of the crack length (c) along the surface, the average ratio being $a/c \sim 1.15$.

2. Crack growth rates along the crack front were derived from the marker load indications. The variation of the growth rate along the crack front was small.

3. Empirical stress intensity factors were deduced from the crack growth rate data. The variation of the geometry correction factor ($K/S\sqrt{\pi a}$) along the crack front was small. The variation of this factor when the crack depth increased from 20 % to 80 % thickness was also relatively small.

4. The crack front near the free surfaces was lagging behind, especially if the maximum stress in the test was high. This can be understood qualitatively as being the result of peak stress alleviation and more crack closure in the plane stress region near the surface.

5. Damage values ($\Sigma n/N$) considerably exceeding 1 were observed for a high peak load stress level and many cycles per flight. Apparently crack growth retardation can also occur during the growth of quarter-elliptical corner cracks. The occurrence of the peak load either at the beginning or the end of the flight had a minor effect on the retardation.

6 REFERENCES

[1] Airplane Damage Tolerance Requirements. MIL-A-83444, Air Force Aeronautical Systems Division, 1974.

[2] S. Minderhoud: Fatigue crack growth of corner cracks. Thesis of the Dep. of Aerospace Eng., Delft Un. of Tech., June 1982.

[3] S. Friedrich: Compilation of test results on corner crack growth in lug specimens under flight-simulation fatigue load. Delft Un. of Tech., Dep. of Aerospace Eng., Document b2-82-20, Dec. 1982.

[4] J. Schijve: Fatigue of lugs. Contributions to the theory of aircraft structures. Nijgh-Wolters Noordhoff Un. Press 1972, pp. 423-440.

[5] I.S. Raju and J.C. Newman, Jr.: Stress-intensity factors for two symmetric corner cracks. Fracture Mechanics, ASTM STP 677, 1979, pp. 411-430.

[6] I.J. Zatz, H.L. Eidinoff and H. Armen, Jr.: An application of the energy release rate concept to crack growth in attachment lugs. AIAA Paper 81-0491, Collected papers, Part I, pp. 402-415, 1981.

[7] T.M. Hsu: Analysis of cracks at attachment lugs. AIAA Paper 80-0753 21st. Structures, Structural Dynamics and Materials Conf., 1980, Part 1, pp. 522-528.

[8] L. Hodulak, H. Kordisch, S. Kunzelmann and E. Sommer. Influence of the load level on the development of part-through cracks. Int. J. of Fracture, Vol., 4, 1978, pp. R33-R57.

[9] H.L. Ewalds and R.J. Furnée: Crack closure measurement along the fatigue crack front of center cracked specimens. Int. J. of Fracture, Vol. 14, 1978, pp. R53-R56.

[10] A.J. McEvily: Current aspects of fatigue. Appendix: Overload experiments. Fatigue 1979 Conf., Un. of Cambridge, March 28-30, 1977.

[11] J.A. Vlasveld and J. Schijve: Tongue-shaped crack extension during fatigue of high strength aluminium alloys. Fatigue of Eng. Materials and Structures Vol. 3, 1980, pp. 129-145.

[12] J. Schijve: Interpolation between calculated stress-intensity factors of semi- and quarter-elliptical cracks. Delft Un. of Tech., Dep. of Aerospace Eng., Report LR-368, Jan. 1983.

[13] J. Schijve: Some formulas for the crack opening stress level. Eng. Fract. Mech., Vol. 14, 1981, pp. 461-465.

Appendix A: K-values derived from results calculated by Raju and Newman

Raju and Newman [5] made finite-element calculations to obtain K-values for quarter-elliptical cracks at open holes and wedge-loaded holes. By superposition as indicated in [5] K-values for pin-loaded holes can then be obtained. The dimensions and relevant stresses are shown below:

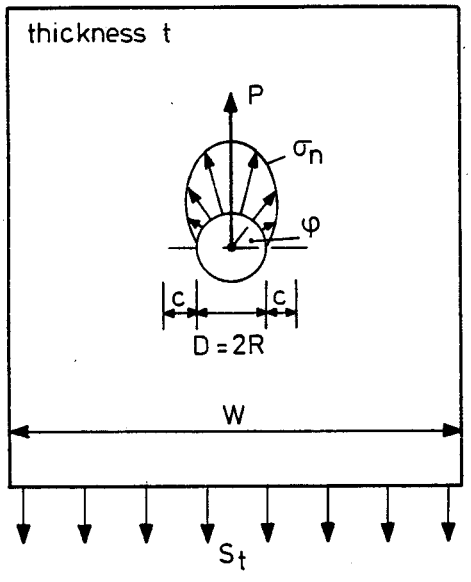

The bearing pressure was supposed to be:

$$\sigma_n = \frac{3P}{4Rt} \sin^2 \varphi \qquad \text{(A1)}$$

The nominal bearing pressure is:

$$S_p = \frac{P}{Dt} \qquad \text{(A2)}$$

The remote tensile stress is:

$$S_t = \frac{P}{Wt} \qquad \text{(A3)}$$

The results in [5] are presented as boundary-correction factors F_t and F_p defined by:

Open hole, S_t applied at upper and lower edge of the panel:

$$K = F_t S_t \sqrt{\pi a/Q} \qquad \text{(A4)}$$

Wedge loaded hole, σ_n applied to upper and lower bore of the hole

$$K = F_p S_p \sqrt{\pi a/Q} \qquad \text{(A5)}$$

a is the crack depth and Q is the shape factor. The superposition equation applying to the pin-loaded hole presented in [5] is:

$$K = \frac{1}{2} S_p \sqrt{\pi a/Q} \left(\frac{D}{W} F_t + F_p\right) \qquad \text{(A6)}$$

which accounts for the equilibrium:

$$D S_p = W S_t \qquad \text{(A7)}$$

Values of F_t and F_p were calculated in [5] for:

a/c = 0.2 1 2

a/t = 0.2 0.5 0.8

R/t = 0.5 1

For the present purpose results are needed for a/c = 1.15, various a/t values and R/t = 1.30. Interpolation between the data of [5] will be necessary, and for R/t = 1.30 it requires extrapolation. The accuracies to be expected for interpolated results were analysed in [12]. Several interpolation procedures were compared, and it turned out that reasonably accurate data may be expected for interpolation between data for different a/c and different a/t values. With respect to extrapolations to the required R/t (= 1.30) the accuracy to be obtained is uncertain. Another source of uncertainty is the width effect because the F_t and F_p values in [5] (*) were calculated for wide panels (large W/D values). In view of these uncertainties interpolations to be made here will be restricted to a/t = 0.2, 0.5 and 0.8 thus avoiding the interpolation step to other a/t values. However, an interpolation between a/c = 1 and a/c = 2 to obtain results for a/c = 1.15 has to be made. According to [12] a linear interpolation between the data of [5] gives the best results. With respect to the extrapolation to R/t = 1.30 it was suggested in [5] that the best results should be expected by considering:

$$\frac{K}{S\sqrt{\pi a/Q}\left\{\sin^2\theta + (a/c)^2\cos^2\theta\right\}^{1/4}} \quad \text{as a linear function of } \sqrt{R/t}$$

Interpolation calculations were made in this way to obtain F_t and F_p values for a/c = 1.15, R/t = 1.30 and a/t = 0.2, 0.5 and 0.8 respectively for polar angles θ = 22.5°, 45° and 67.5°.

The calculated results apply to very wide panels with two symmetric edge cracks. For the open hole under tension a width correction factor was proposed by Newman [5]

$$F_W = \left[\sec\left(\frac{\pi R}{W}\right)\sec\left(\frac{\pi(R+c)}{W}\sqrt{\frac{a}{t}}\right)\right]^{1/2} \qquad \text{(A8)}$$

and he suggested (private communication) that it might be adopted for the wedge-loading case as well. A second correction should be made for the presence of only one corner crack instead of two symmetric cracks. For this purpose the Shah correction factor is adopted:

$$F_{2\to1} = \sqrt{\frac{D+\pi ac/4t}{D+\pi ac/2t}} \qquad \text{(A9)}$$

With these two correction factors the superposition equation (A6) becomes:

$$\frac{K}{S_p\sqrt{\pi a}} = \frac{F_W F_{2\to1}}{2\sqrt{Q}}\left(\frac{D}{W}F_t + F_p\right) \qquad \text{(A10)}$$

Calculated results are plotted in Figure 11.

(*) Values of F_p for a/c = 2 and a/t = 0.2 and 0.5 presented in [5] are incorrect as Dr. Newman reported by correspondence. He supplied the corrected data.

Appendix B: Analysis of the constant-amplitude crack growth life

It is not logical to plot the three CA results as one single S-N data set because neither S_m nor R is the same for all data. However, the difference between R-values can be accounted for by considering the effect of R on ΔK_{eff}. For this purpose the U-relation is drawn from [13]

$$U = \Delta K_{eff}/\Delta K = 0.55 + 0.33\ R + 0.12\ R^2 \qquad (B1)$$

The crack growth life can be obtained by integration of:

$$da/dn = \alpha\ (\Delta K_{eff})^{\beta} \qquad (B2)$$

with $\beta = 2.75$ applicable to the present results (see Eq. 2). Combining (B1) and (B2):

$$dn = (1/\alpha)\ (\Delta K_{eff})^{-\beta}\ da = (1/\alpha)\ (U\Delta K)^{-\beta} = (1./\alpha)\ [U\ C(a)\ \Delta S\ \sqrt{\pi a}]^{-\beta} da \qquad (B3)$$

with C(a) as the geometry correction factor. Actually Eq. (B3) applies to a through crack, but da/dn did not vary significantly along the crack front of the corner cracks, while a/c did not deviate very much from 1. Consequently (B3) should give approximately correct indications. Integration leads to:

$$N_t - N_2 = \int dn = \frac{1}{\alpha}\ (U\Delta S)^{-\beta} \int_{a_{initial}}^{a_{failure}} [C(a)\ \sqrt{\pi a}]^{-\beta}\ da \qquad (B4)$$

In the present case $a_{initial}$ = 2 mm, but $a_{failure}$ is unknown and will depend on S_{max}. However, when $a \rightarrow a_{failure}$ the crack rate is very high, and a somewhat different $a_{failure}$ will hardly affect the crack growth life. As a result the integral in (B4) will be approximately constant for different CA-load cycles. Equation (B4) then implies:

$$\frac{\left(N_t - N_2\right)_{test\ 1}}{\left(N_t - N_2\right)_{test\ 2}} \approx \left(\frac{U_1\ \Delta S_1}{U_2\ \Delta S_2}\right)^{-2,75} \qquad (B5)$$

With this equation and the U(R) relation in Eq. (B1) the following results were obtained:

Specimens	S_{max} S_{min} MPa	R	ΔS MPa	U	$N_t - N_2$ (cycles) Av.test result	Prediction	Ratio
2, 3	120 40	1/3	80	0.673	11726	11726 (by def.)	1 (by def.)
17, 19	160 0(*)	0	160	0.55	2959	3036	0.97
10, 18	200 0	0	200	0.55	2481	1644	1.51

(*) S_{min} = - 40, but a compressive load does not pass through the critical net section.

The mean life of specimens 2 and 3 was used as a reference value (test 1 in Eq. B5), from which the life for the other specimens was predicted. The prediction for the crack growth life of specimens 17 and 19 deviates only 3 % of the test result, and that is an excellent prediction. For specimens 10 and 18 the test result is 1.5 times the prediction. It is difficult to explain this fairly large deviation.

Loading	Specimen No.	Stress (MPa) S_{max}/S_{min}	Life (kc) Upper lug N_2/N_t	Lower lug N_2 / N_t	$N_t - N_2$ (kc) Upper lug	Lower lug	Mean (log)
CA	2	120/40	31.5/42.269	29.0/41.817	10.769	12.817	11.726
	3	120/40	19.5/30.815	19.8/31.906	11.315	12.106	
	17	160/-40	5.8/8.418	5.3/7.732	2.618	2.432	2.959 (a)
	19	160/-40	8.5/11.8	9.2/14.805	3.3	5.605	
	10	200/0	3.644/6.195	5.5/7.911	2.551	2.411	2.481 (a)
	18	200/0	1.0/4.390	0.2/2.476	3.390	2.276	
II		$S_g/S_{OL}/m$					
	4	-40/160/5	29/37.112	24/33.357	13.112	9.357	11.077
	5	-40/160/100	55/71.602	57/73.302	16.602	16.302	16.451
	11	-40/200/5	18/25.692	17.3/24.907	7.692	7.607	7.649
	9	-40/200/100	126/156.502	95.75/133.001	30.502	37.251	33.708
III	6	-40/160/5	15/20.726	19/25.596	5.726	6.596	6.598
	13	-40/160/5	21.9/28.913	14.5/21.653	7.013	7.153	
	7	-40/160/100	43.25/57.201	61.25/77.902	13.951	16.652	15.242
	14	-40/200/5	14.7/23.867	14/21.661	9.167	7.661	8.632
	16	-40/200/5	14/22.506	28.567/37.863	8.506	9.296	
	8	-40/200/100	144.701/174.702	64.5/92.701	30.001	28.201	29.087
	15	0/200/100	79.1/112.002	71.1/109.001	32.902	37.901	35.313
	20	-80/200/100	62.0/13.801	78.0/103.402	31.801	25.402	28.422

Table 1: Survey of fatigue lives

(a) median in view of one exceptional result

Type of loading	S_g (MPa)	Life (cycles)		Σn/n-values			
				S_{OL}=160		S_{OL}=200	
		Predicted	Test	m=5	m=100	m=5	m=100
II	-40	7363	11077	1.5			
		11389	16451		1.4		
		6719	7649			1.1	
		11305	33708				3.0
III	-40	7363	6598	0.9			
		11389	15242		1.3		
		6719	8632			1.3	
		11305	29087				2.6
	0	11305	35313				3.1
	-80	11305	28422				2.5

Table 2: Predicted lives, test results and Σn/N-values.

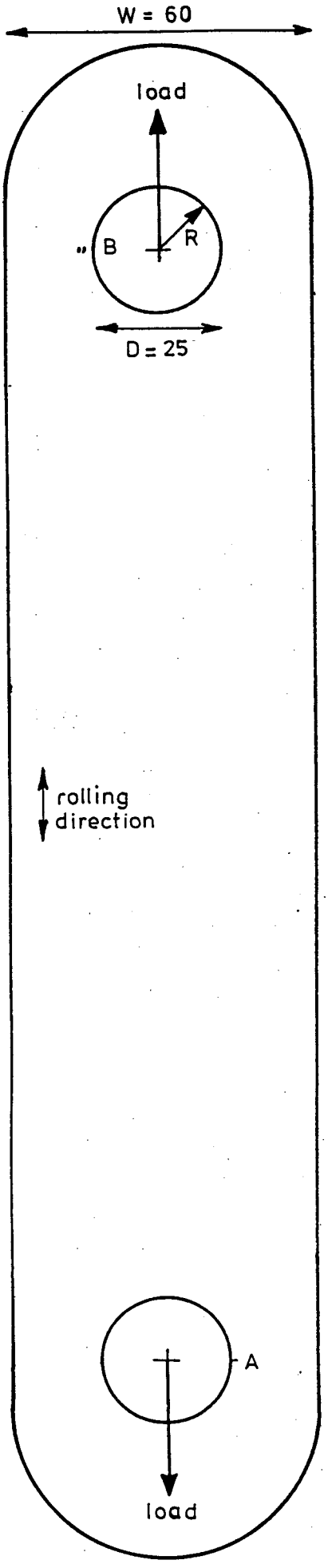

All dimensions in mm

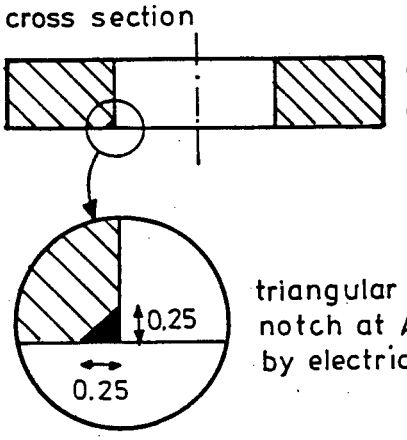

Material properties	
7075 - T6	S_u = 568 MPa
	$S_{0.2}$ = 506.5 MPa
	δ (50 mm) = 13.5 %

Survey of tests (stress in MPa)					Specimen No.
CA		$S_{min} = 40$, $S_{max} = 120$			2,3
		$S_{min} = -40$, $S_{max} = 160$			17, 19
		$S_{min} = 0$, $S_{max} = 200$			10, 18
Type II	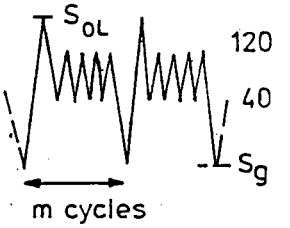	S_g	S_{OL}	m	
		-40	160	5	4
				100	5
			200	5	11
				100	9
Type III		-40	160	5	6,13
				100	7
			200	5	14.16
				100	8
		0			15
		-80			20

$K_t \approx 2.8$

Figure 1: Specimen dimension, material properties and surv y of tests.

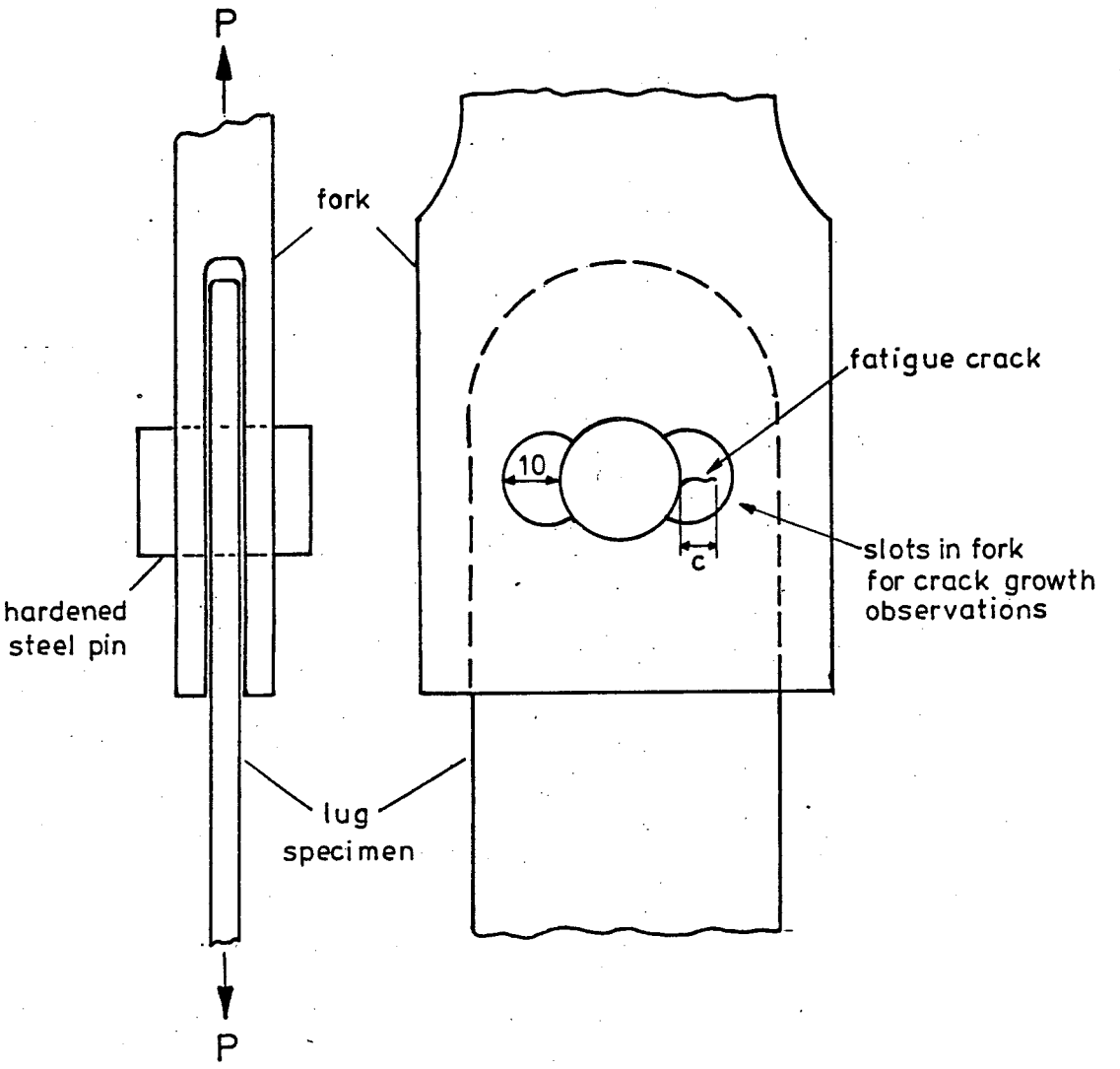

Figure 2 Fork for loading the lug ends

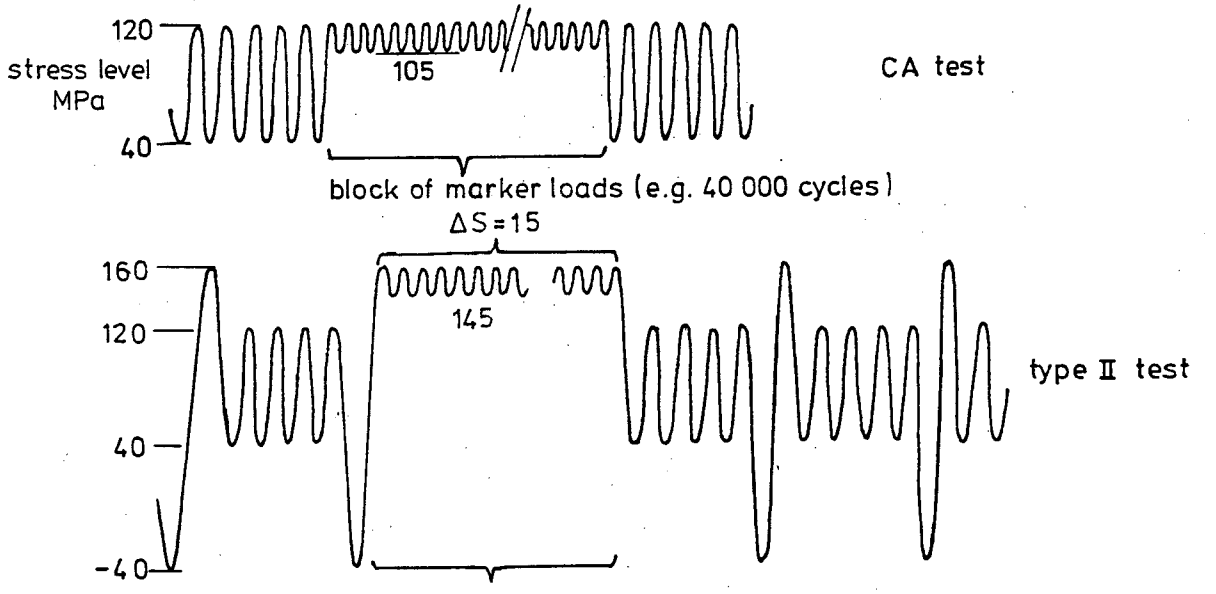

Figure 3. Marker load cycles

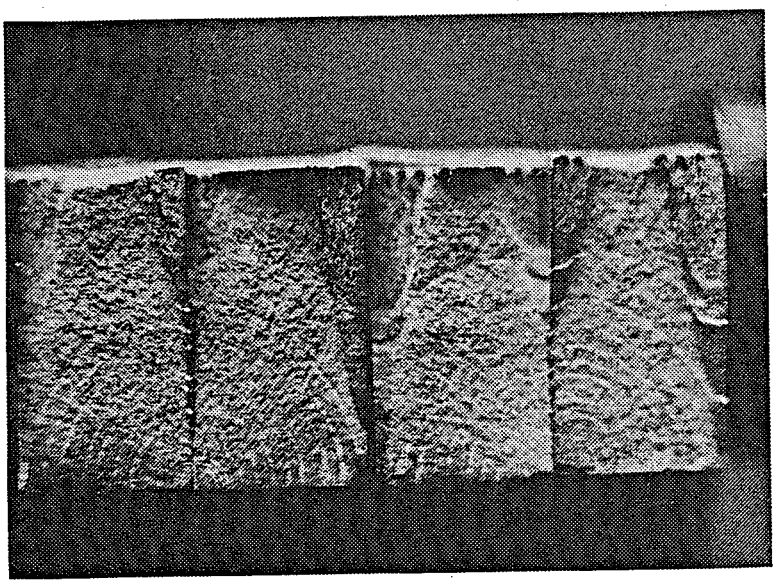

Figure 4: Marker load indications on the fracture surfaces of specimen No. 13 (load history of type III)

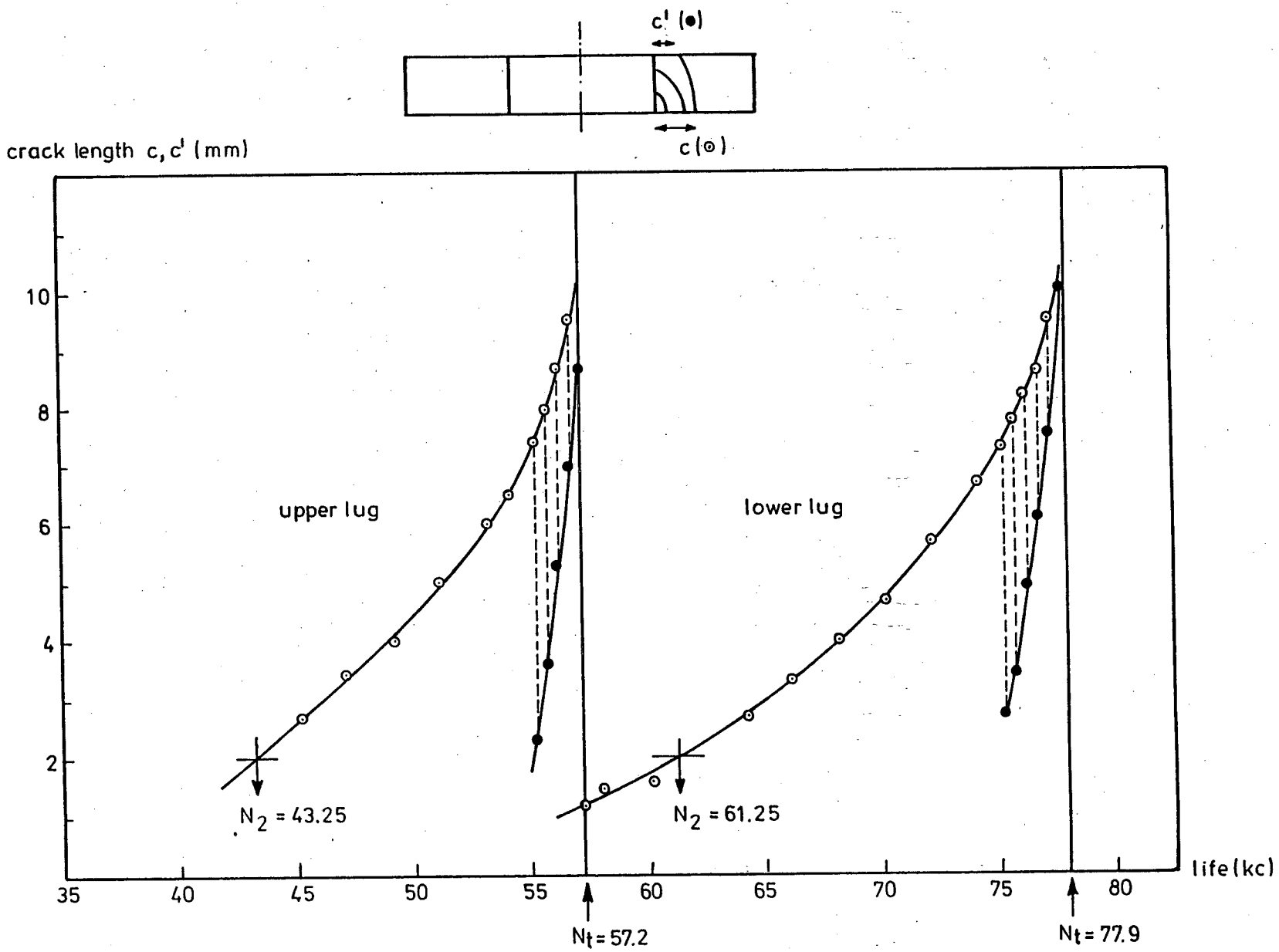

Figure 5: Visual crack growth observations from one specimen (No. 7)

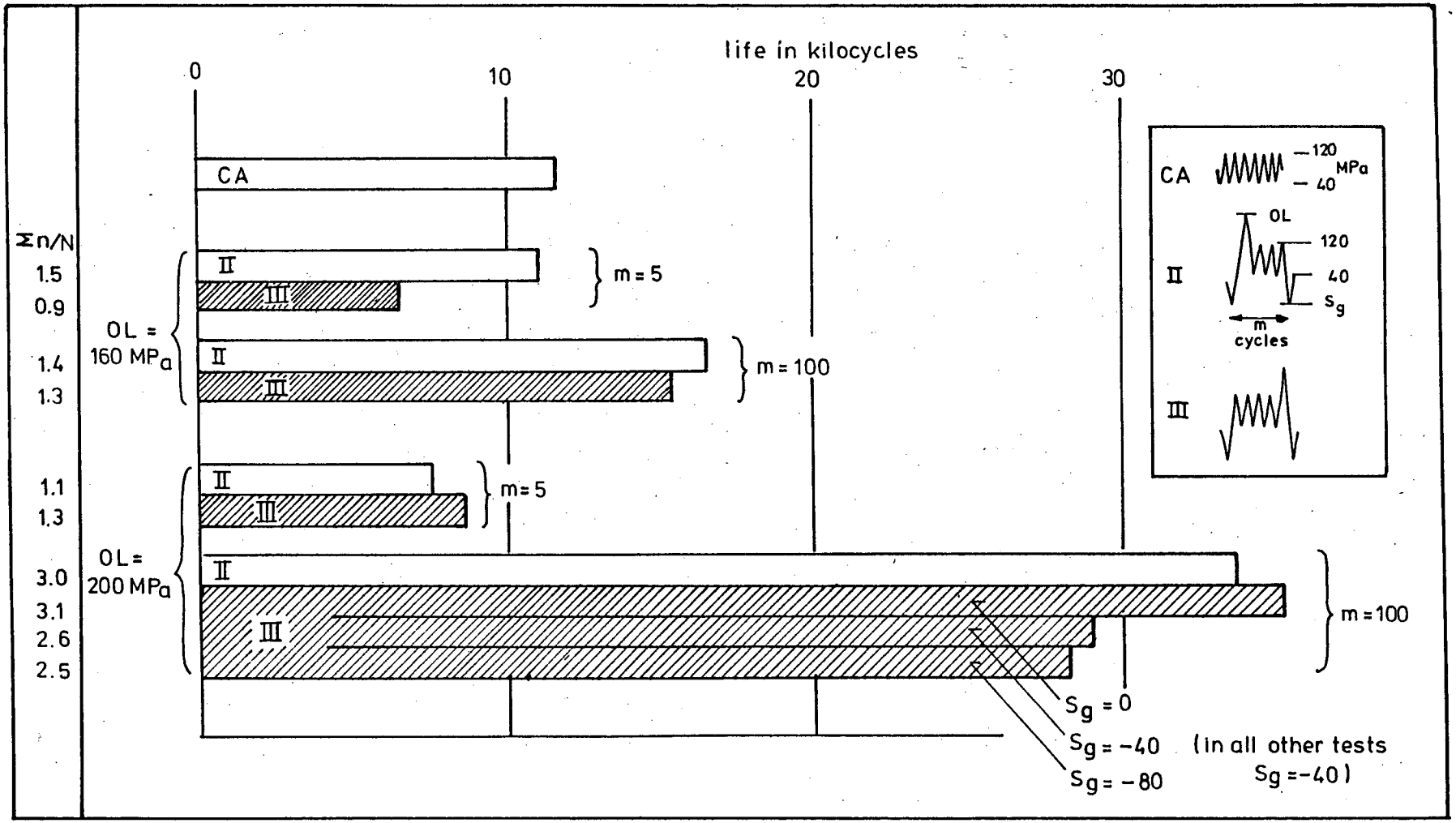

Figure 6: Survey of test results. Comparison between CA, II and III, and between m = 5 and m = 100.

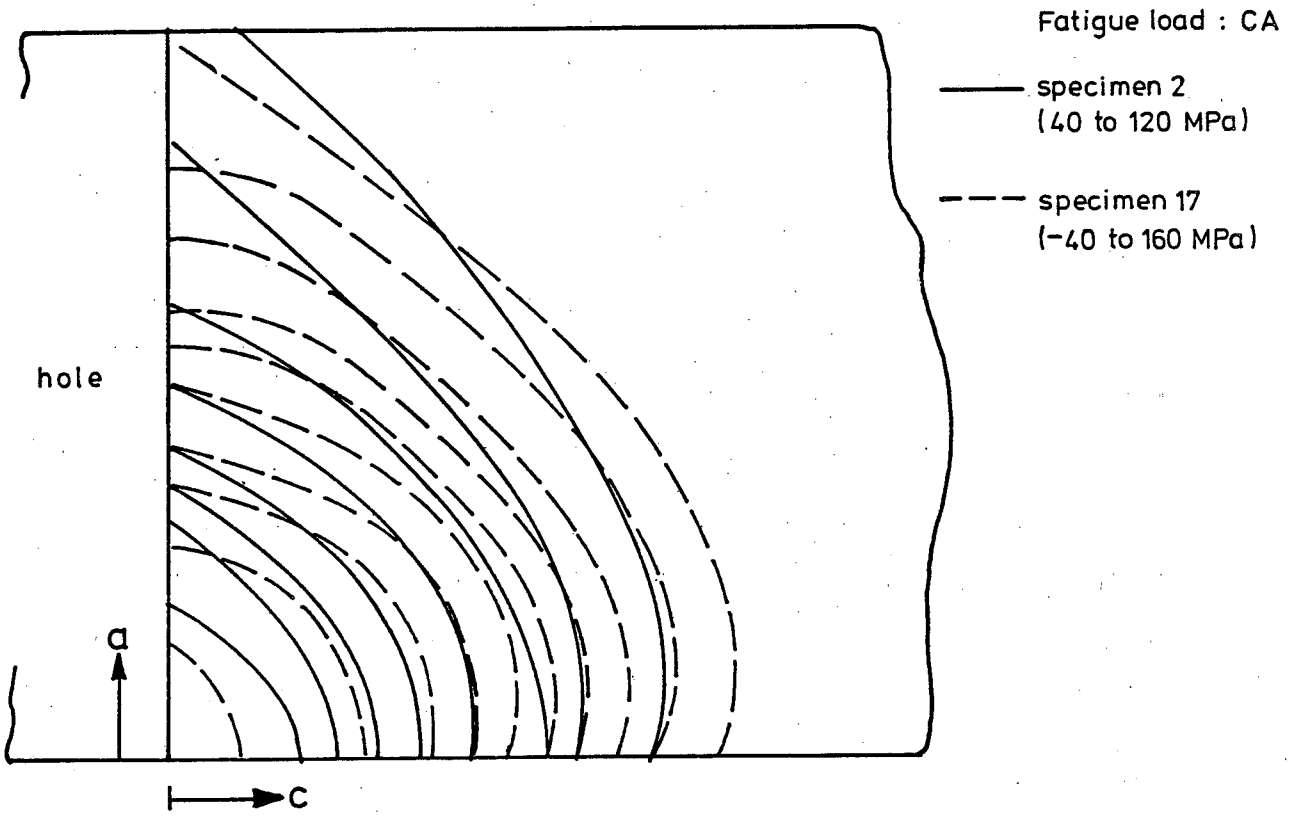

Fig.7a

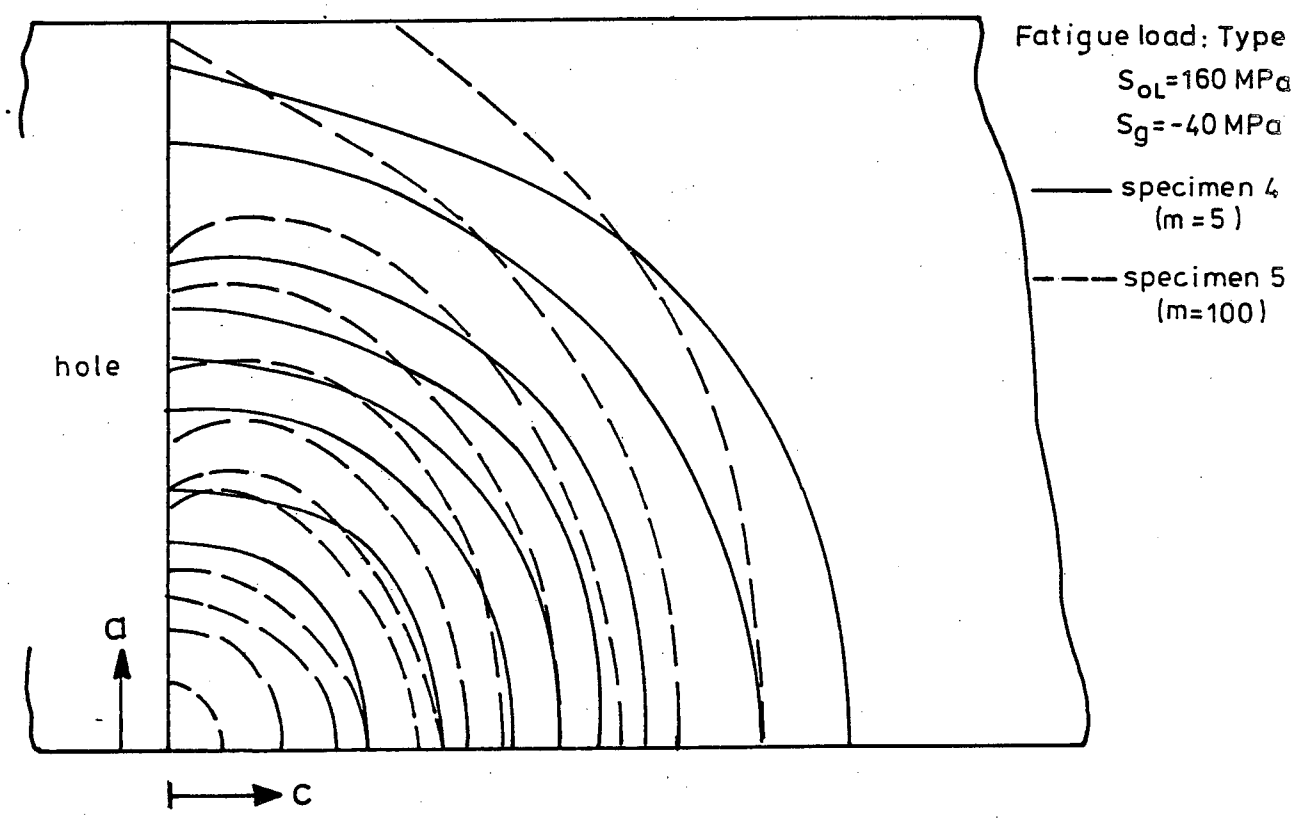

Fig.7b

Figure 7: Crack front location observed from marker load indications

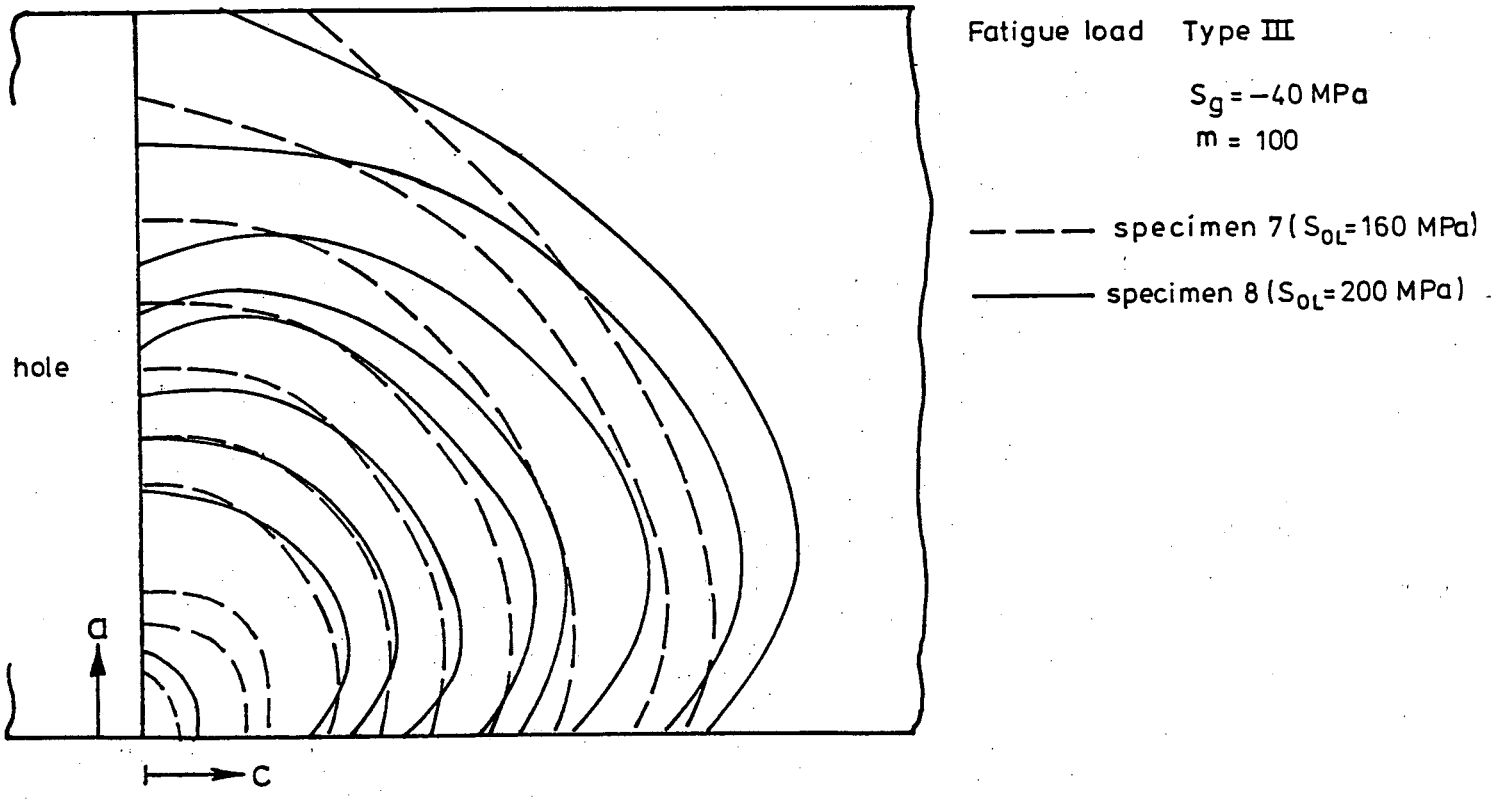

Fig. 7c

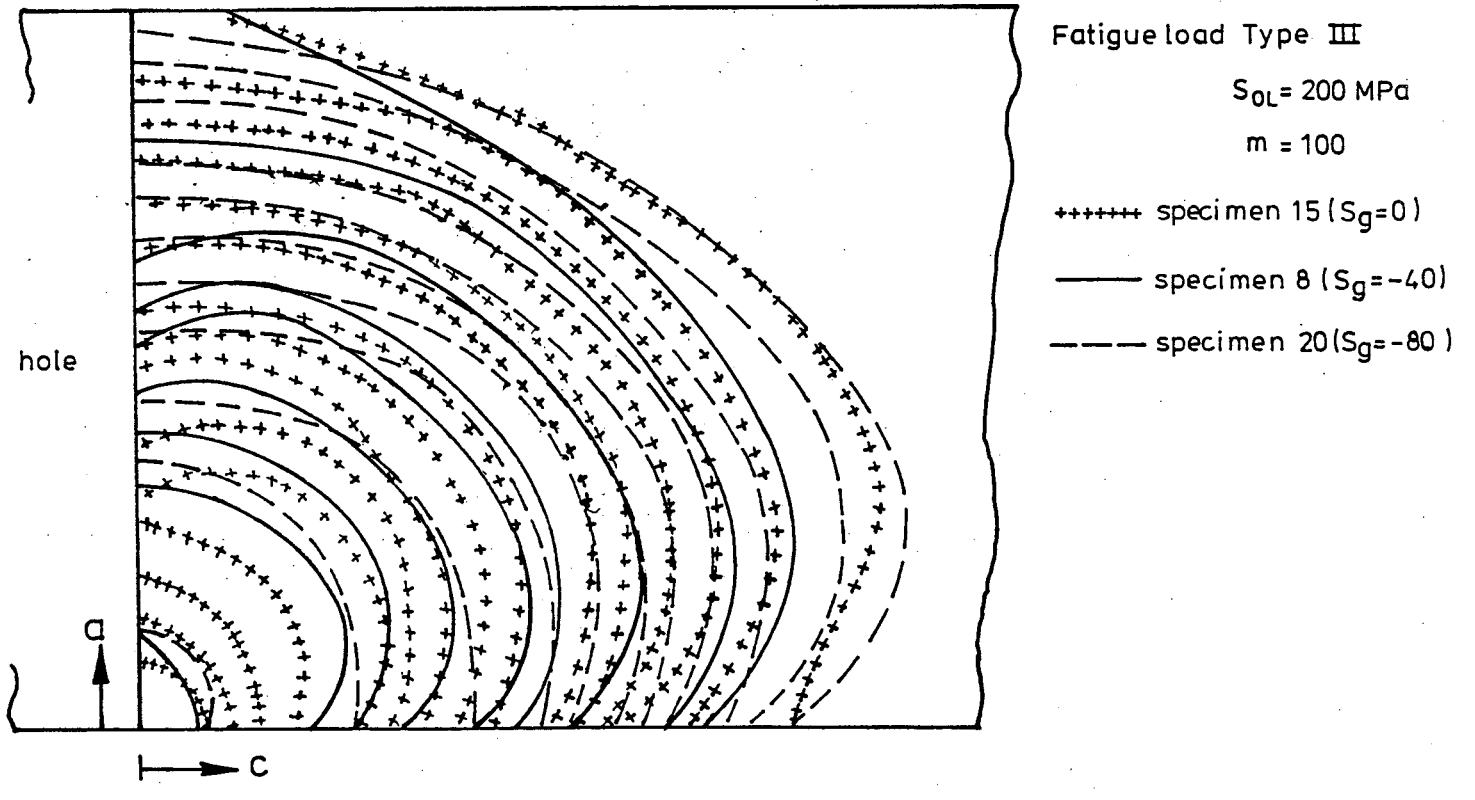

Fig. 7d

Figure 7 (continued)

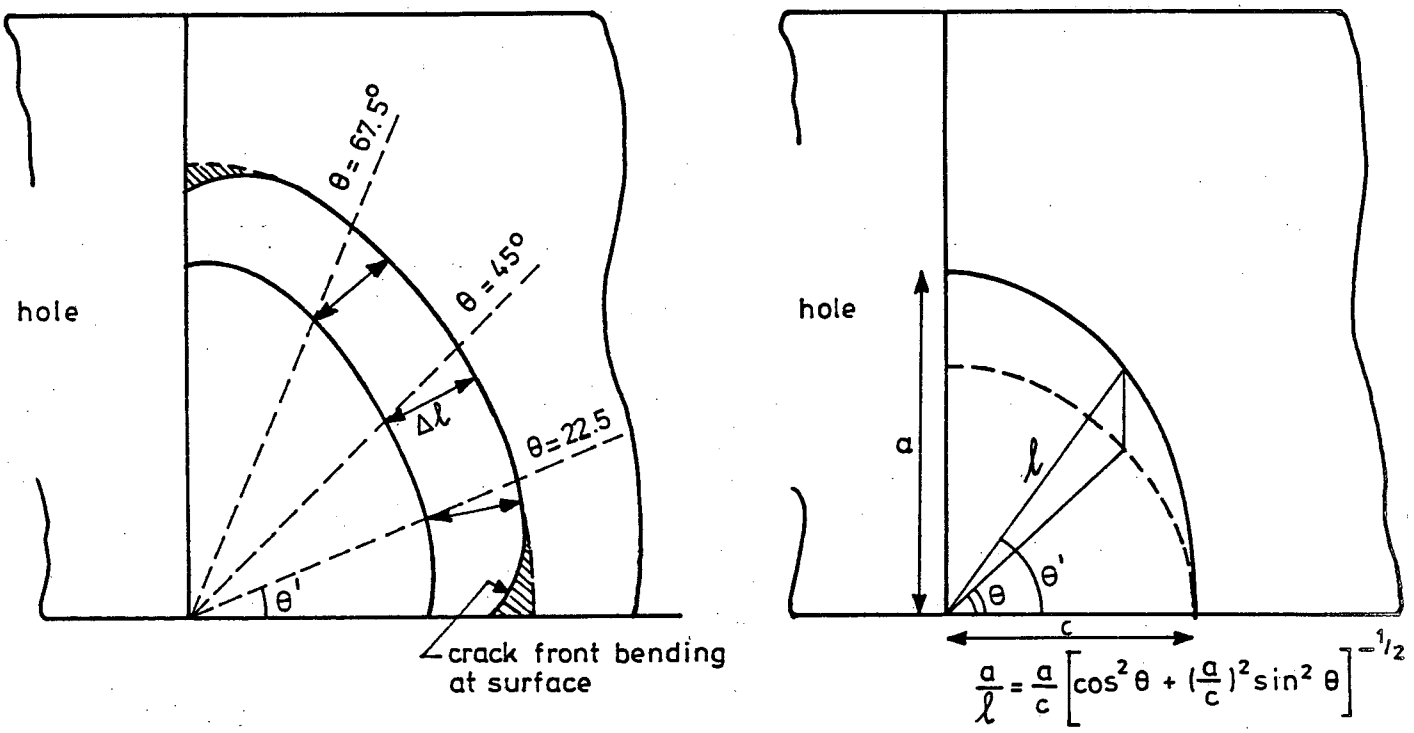

Figure 8: The crack extension is measured perpendicular to the crack front

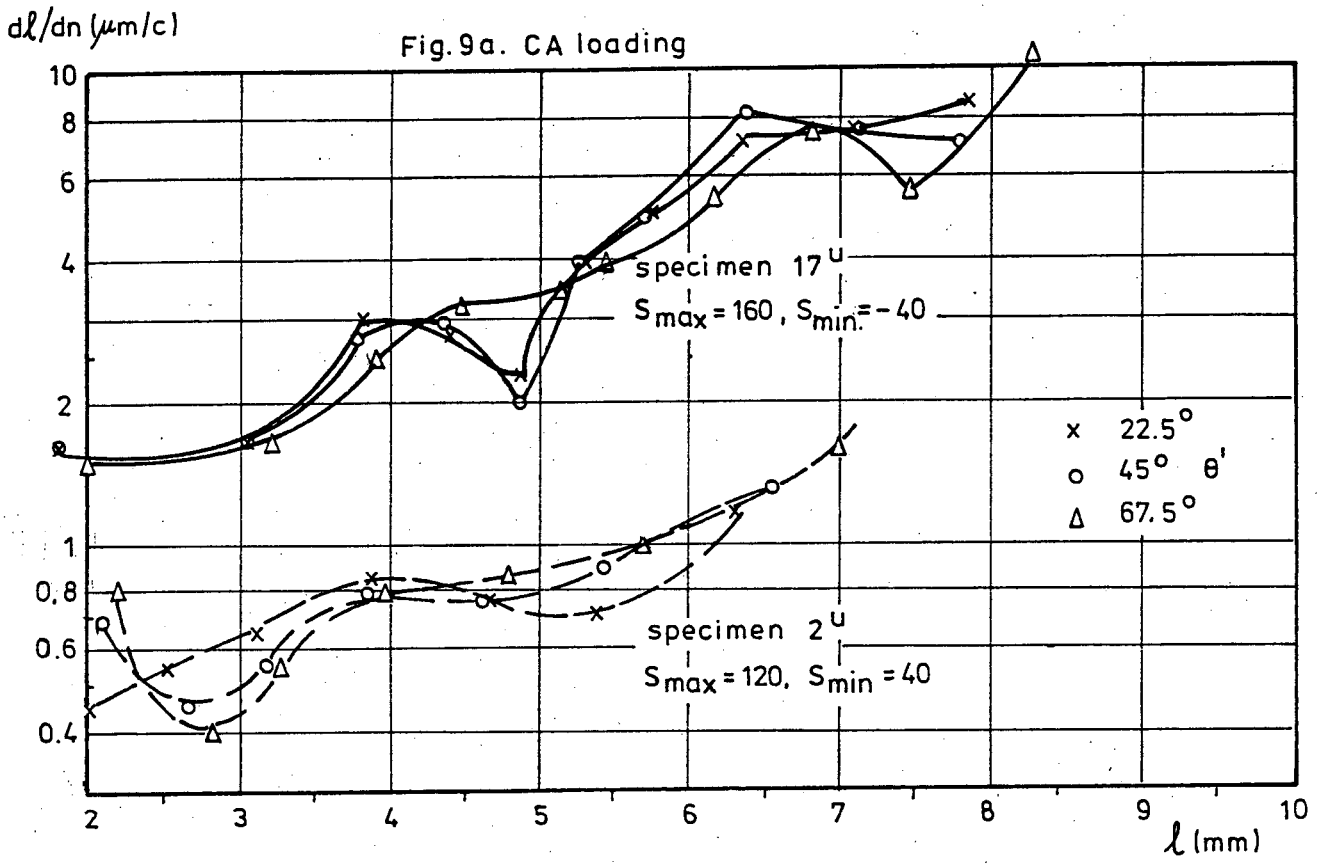

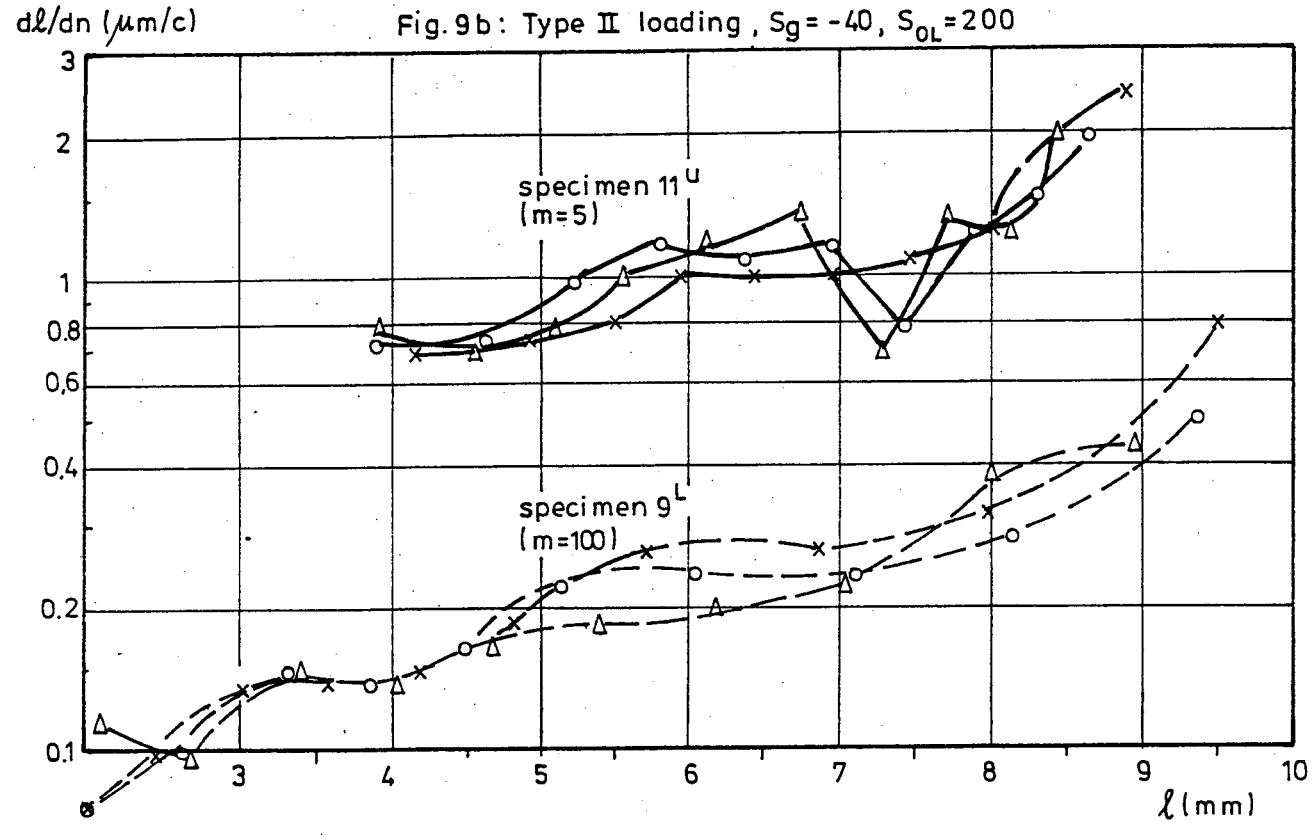

Figure 9: Crack growth rate data derived from the marker load

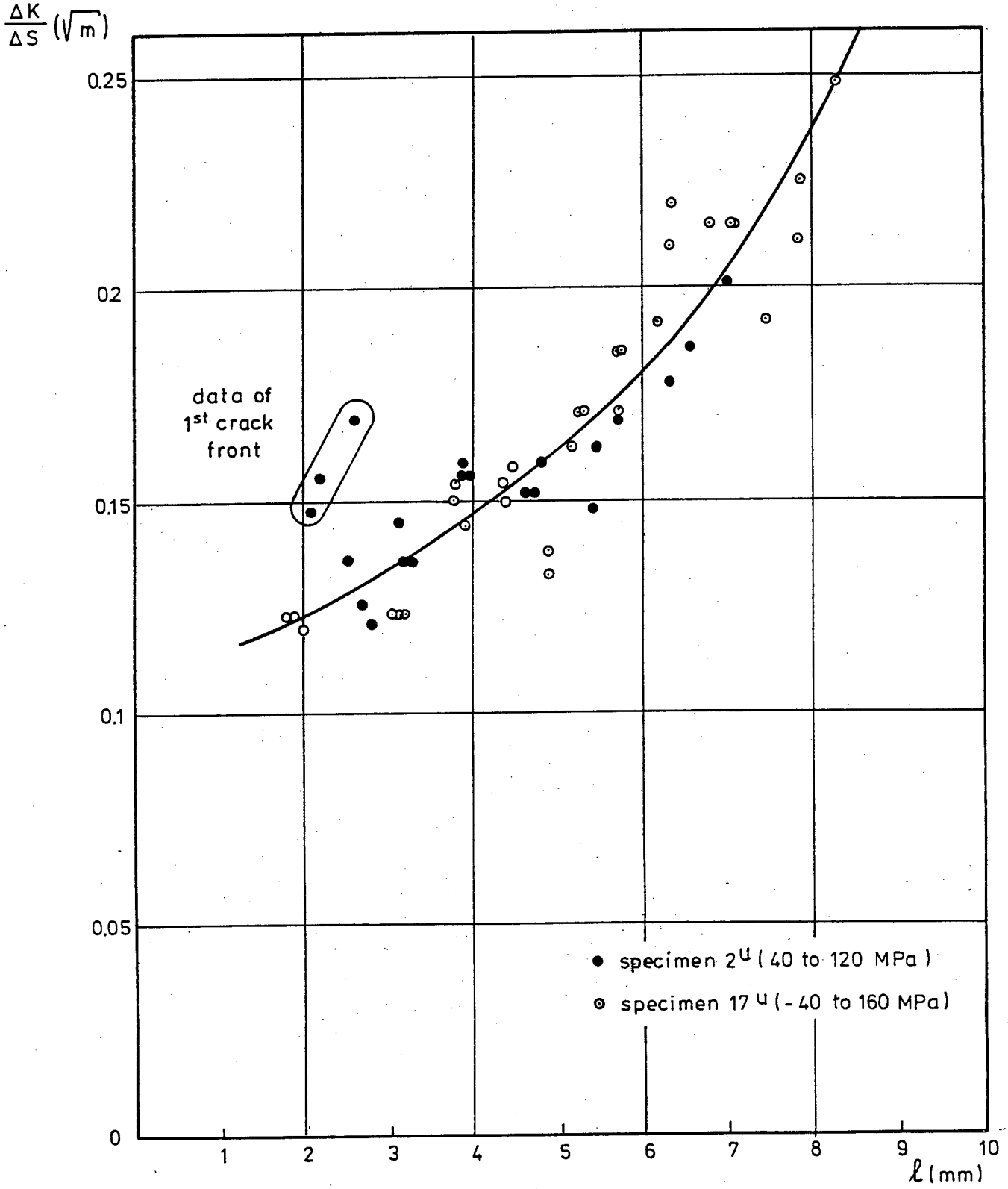

Figure 10: Empirical ΔK/ΔS-value- derived from the da/dn data in Figure 9a (CA-loading)

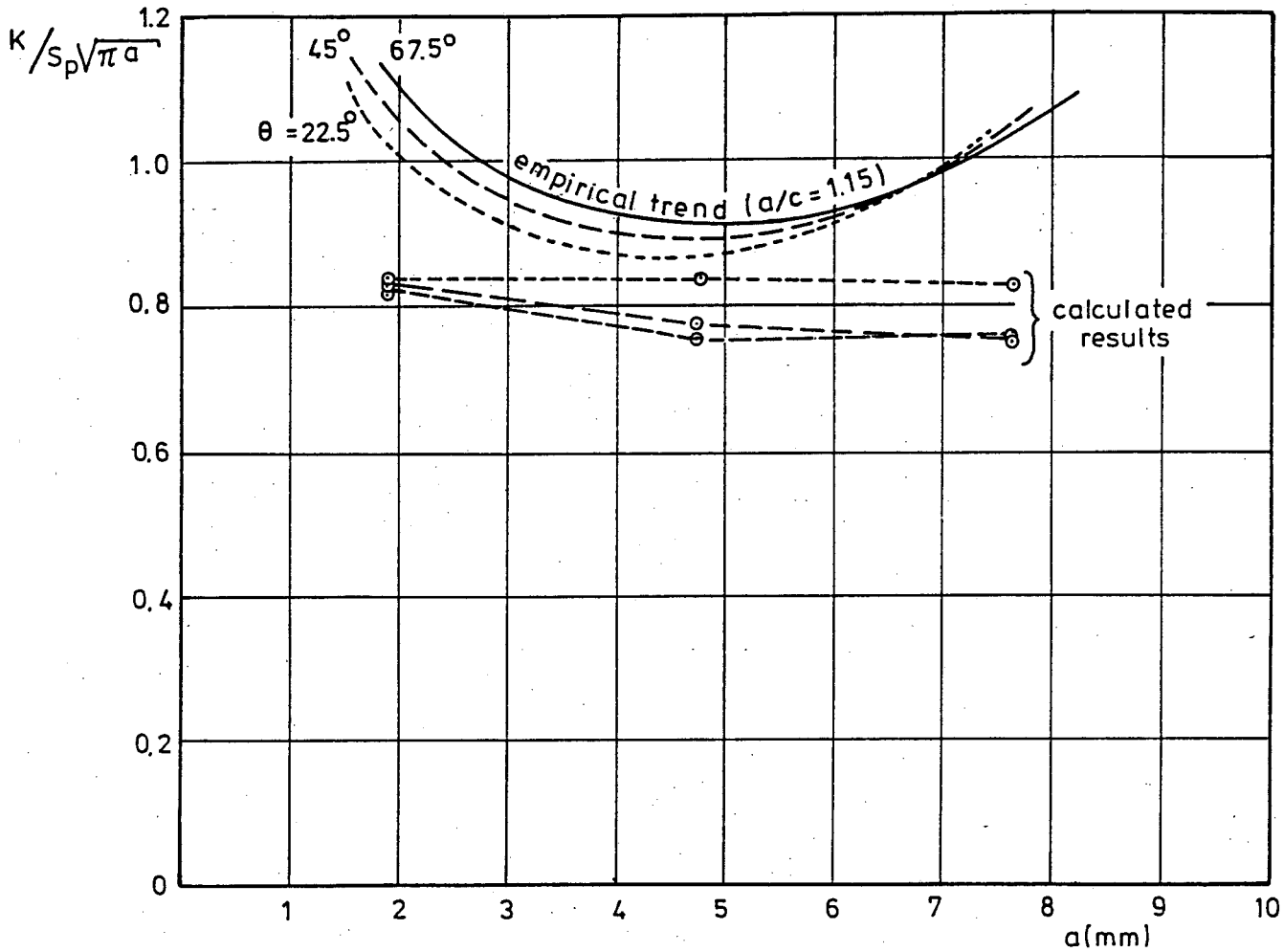

Figure 11: The average empirical curve of Fig. 10 converted into $K/S_p\sqrt{\pi a}$ as a function of a.